Taylor & Francis
Taylor & Francis Group

International Journal of Occupational Safety and Ergonomics

ISSN: (Print) (Online) Journal homepage: https://www.tandfonline.com/loi/tose20

Security cameras in taxicabs with three rows of seating

Shengke Zeng

To cite this article: Shengke Zeng (2022) Security cameras in taxicabs with three rows of seating, International Journal of Occupational Safety and Ergonomics, 28:1, 562-571, DOI: 10.1080/10803548.2020.1817651

To link to this article: https://doi.org/10.1080/10803548.2020.1817651

Published online: 09 Oct 2020.

International Journal of Occupational Safety and Ergonomics (JOSE), 2022
Vol. 28, No. 1, 562–571, https://doi.org/10.1080/10803548.2020.1817651

Security cameras in taxicabs with three rows of seating

Shengke Zeng *

National Institute for Occupational Safety and Health, Centers for Disease Control and Prevention, USA

Taxicab security cameras are widely used to deter crimes against taxicab drivers in two-row-seating taxicabs. Some of these cameras have difficulty for use in three-row-seating taxicabs due to increased distance between the camera and the third-row seats. This project tested five sample taxicab security cameras with different image-sensor pixel counts to determine their utility for three-row-seating taxicabs. The cameras videotaped a normalized camera resolution test chart mounted in the third-row seat of a simulated three-row-seating taxicab in both daylight and dark (with infrared radiation) conditions. The resolution of each camera was measured and compared with the resolution threshold for customer facial identification. A dome-mounted camera with a standard-definition image-sensor is suggested as an effective camera in sustaining high camera resolution with small data file size for facial identification in the third-row seats. The image-sensors with at least 1280 × 720 pixels are suggested for windshield-mounted cameras in three-row-seating taxicabs for facial identification.

Keywords: taxicab-driver homicide; taxicab security cameras; three-row-seating taxicabs; camera resolution; facial identification; computer facial recognition

1. Introduction

Taxicab drivers are more likely to be victims of homicide than workers of many other industry sectors. Based on data from the Bureau of Labor Statistics, the homicide rate in the taxi and limousine service (2.03 per 100,000 workers) was seven times greater than that of all workers (0.29 per 100,000 workers) [1,2]. A National Institute for Occupational Safety and Health (NIOSH) epidemiology study showed that cities with taxicab security cameras experienced a significant reduction in taxicab-driver homicides [3]. NIOSH engineering studies quantified the camera resolution requirement for a taxicab security camera to provide sufficient customer facial detail for customer facial identification [4,5]. This camera resolution threshold could be applied to the security cameras used in different types of taxicabs, including three-row-seating taxicabs, such as minivans and SUVs, which have become popular in the taxi industry. The three-row-seating taxicabs have distinguishable geometric differences in the cab length with an additional distance from the second-row seats to the third-row seats. This added distance causes the camera resolution of a windshield-mounted camera to deteriorate in the third-row seats. Some market-available taxicab security cameras, which are designed to meet the minimum camera resolution requirement for a two-row-seating taxicab, might not necessarily meet the same camera resolution requirement for the third-row seats in a three-row-seating taxicab due to the extended camera-to-customer distance. It was necessary to evaluate the camera resolution performance of taxicab security cameras in the third-row seats in a three-row-seating taxicab.

Currently, there is no peer-reviewed published literature evaluating the technical effectiveness of taxicab security cameras in three-row-seating taxicabs for safety or crime deterrence. In addition, there is no national standard or guidance document for selecting taxicab security cameras in the USA. Only a few domestic and international cities/states have issued specifications, reports or guidance documents for taxicab security cameras [6–12], none of which have any minimum performance requirements for three-row-seating taxicabs.

In order to investigate the camera resolution performance of taxicab security cameras in a three-row-seating taxicab, five taxicab security cameras that were likely to meet minimum camera resolution requirements in the third-row seats were acquired for camera tests in two extreme light conditions.

2. Methods/procedures

2.1. *Procedures of security camera resolution tests in three-row-seating taxicabs*

The test procedures were designed to evaluate the camera resolution of sample security cameras in the third-row seats of a simulated three-row-seating taxicab for their compliance with the minimum camera resolution requirements.

*Email: szeng@cdc.gov

Five sample taxicab security cameras with different image-sensor pixel counts, mounted on the windshield or the ceiling of the simulated taxicab, recorded in-cab images with a specially designed normalized camera resolution test chart mounted in a third-row seat. The camera resolution compliance was tested in two extreme light conditions, bright sunny daylight and dark conditions with infrared (IR) light-emitting diode (LED) radiation. In the post-test data analysis, the test chart images were retrieved from the captured cab images and the camera resolution was measured by photographic quality test software. Each measured camera resolution was compared with the camera resolution requirement for customer facial identification, which was determined in a previous taxicab security camera study [5]. The camera resolution was also compared with the camera resolution threshold for computer facial recognition.

2.2. *Selection of taxicab security cameras for evaluation*

Five taxicab security cameras were selected for this study. Four of the cameras were available on the US market, and one was a prototype camera acquired from a taxicab security camera manufacturer. Cameras C1 and C2 had full high-definition (FHD) image-sensors (1920 × 1080 pixels). Camera C3 had a high-definition (HD) image-sensor (1280 × 720 pixels). Camera C4 had dual standard-definition image-sensors (2 × 720 × 572 pixels), with one wide-angle lens focused on the front-seat customer/driver and one telephoto lens focused on the rear-seat customers. Camera-group C5 consisted of a standard-definition primary camera focused on the first-row and second-row seats, and a standard-definition secondary dome-mounted camera focused on the third-row seats. The pixel count of the primary camera image-sensor was 720 × 584 pixels and for the dome camera was 976 × 494 pixels. The features of cameras C1–C5 are presented in Table 1.

2.3. *Normalized camera resolution and resolution thresholds*

To assess a taxicab security camera's photographic capability, a previous taxicab security camera evaluation conducted by the NIOSH determined the 'normalized' camera resolution threshold for a taxicab security camera for effective in-cab customer facial identification [5]. The normalized camera resolution of a taxicab security camera determines the amount of facial detail of an in-cab customer in either the front or back seat positions. The normalized camera resolution in this study was defined as the 'number of linewidths per head height (LPHH)' [4,5]. The head height was defined as 25.5 cm, which is the head height (from the menton to the top of the head) of a 99th-percentile male [13]. With the same normalized camera resolution, when a customer sits in a front or back seat, his/her head image would contain an equal amount of facial detail. The normalized camera resolution varies inversely with the distance between the camera and the customer face, hence, the camera resolution in the third-row seat would contain fewer LPHH than that in the front seat. When a security camera is used in a three-row-seating taxicab, the camera usually needs a higher pixel-count image-sensor than in a two-row-seating taxicab in order to maintain the normalized camera resolution on or above the resolution threshold in all three rows of the seats. The normalized camera resolution threshold for facial identification was determined in the previous taxicab security camera study as 47.7 LPHH [5]. The normalized camera resolution threshold for computer facial recognition was determined as 64 vertical pixels with monochrome color [14]. The vertical monochrome pixels could be converted to an equal number of linewidths (64 LPHH) in this camera resolution comparison [15].

2.4. *Normalized camera resolution test chart and resolution measurement*

A normalized camera resolution test chart, as shown in Figure 1, contains a slanted-edge dark stripe that was designed to measure image resolution [16–18]. In order to measure normalized camera resolution, the height of the chart was designed as 25.5 cm, which is the head height of a 99th-percentile male [13]. After the taxicab images were videotaped by the sample cameras, the test chart image was retrieved from the video clips and Imatest Master (Version 4.1.8) photographic quality test software was used to determine the camera resolution. Camera resolution is

Table 1. Features of sample cameras.

Camera	Image-sensor type	Lenses	Image-sensor pixel count (primary)	Image-sensor pixel count (secondary)
1	Full high definition	Single	1920 × 1080	–
2*	Full high definition	Single	1920 × 1080	–
3	High definition	Single	1280 × 720	–
4	Standard definition	Dual	720 × 572, wide angle	720 × 572, telephoto
5	Standard definition	Dual	720 × 584	976 × 494, dome

Note: * Prototype camera.

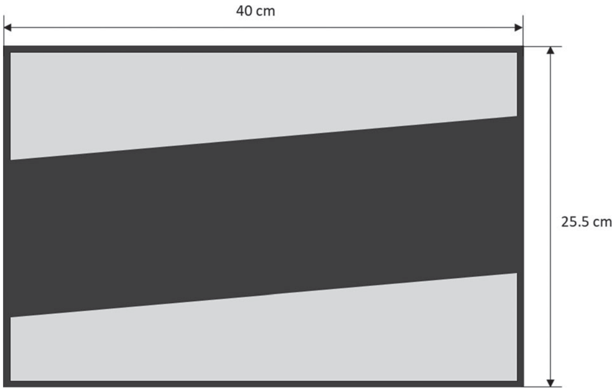

Figure 1. Normalized camera resolution test chart.

determined by measuring the modulation transfer function (MTF) or spatial frequency response (SFR) of the slanted-edge image. The MTF or SFR is a transfer function commonly used for defining the spatial resolution of an imaging system [16,19–22], such as a taxicab security camera. The camera resolution of the test chart was determined as the spatial frequency of the measured MTF falls to 50% from its peak. The unit of the normalized camera resolution is LPHH as the height of the test chart is 25.5 cm.

2.5. *Test setup*

The taxicab security camera tests were conducted in a simulated three-row-seating taxicab. The overall taxicab seating configuration and dimensions are shown in Figure 2. All of the sample cameras, except the dome camera of camera-group C5, were mounted on the windshield near the rear-view mirror. The distance between the front cameras and the test chart was 238 cm. The dome camera of C5 was mounted on the ceiling of the vehicle near the second-row seat and was 80 cm from the normalized camera resolution test chart mounted in the middle of the third-row seat. At this position, the camera's angle of view (81.2°) could cover all of the third-row-seating customers. The test chart was mounted 21.3 cm in front of the head rest of the third-row middle seat, which is the head length of a 99th-percentile male [13].

2.6. *Camera resolution tests in two extreme light conditions*

The resolution performance of the five sample cameras were tested in two extreme light conditions measured in lux (the International System of Units derived unit of illuminance, 1 lux = 1 lumen/m^2): L1, sunny daylight (100,000 lux or above); L2, moonless dark (0–2 lux, with only IR radiation from the camera's built-in IR LEDs). The test chart was indirectly illuminated by sunny daylight in condition L1 and was radiated by each camera's IR LEDs in condition L2. Each camera captured a set of at least five video frames of cab images in each of the two light conditions. The mean resolution in condition L1, mean resolution in condition L2 and total-mean resolution in both conditions L1 and L2 were measured with Imatest Master, and then compared with the normalized camera resolution threshold for facial identification. These normalized mean camera resolutions were also compared with the monochrome camera resolution threshold for computer facial recognition. A camera passed the test if its mean camera resolution was equal to or exceeded each of the two resolution thresholds.

3. Results

Five taxicab security cameras were tested to measure their normalized camera resolution (referred as 'camera

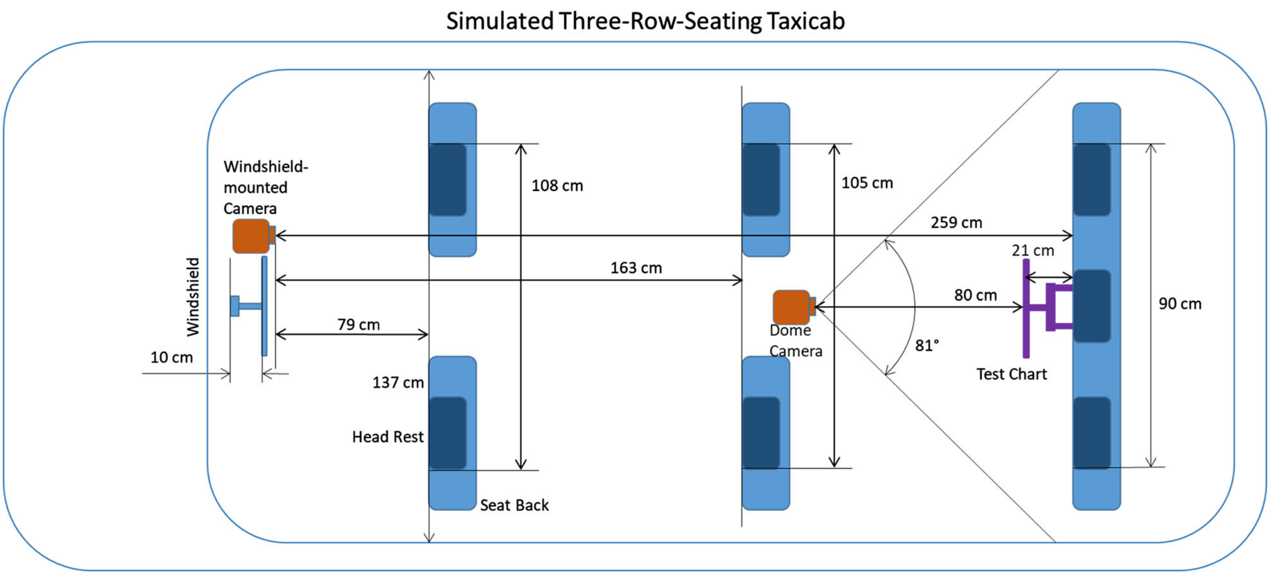

Figure 2. Camera and test chart position inside the simulated three-row-seating taxicab.
Note: The full color version of this figure is available online.

resolution') in the third-row seat in conditions of both daylight (L1) and dark with IR radiation (L2). Starting with the camera that has the lowest camera resolution, Figures 3–7 illustrate the sample cab images captured by the five sample cameras (C1–C5), with different image-sensor pixel counts. As shown in Figure 3, camera C4 with dual standard-definition image-sensors captured the image that yielded the lowest camera resolution of 37.9 LPHH in dark conditions. Camera C3 with an HD image-sensor measured a resolution of 47.6 LPHH in the image shown in Figure 4. This resolution was close to the resolution threshold of 47.7 LPHH for facial identification. Figures 5 and 6 illustrate the camera resolutions of 58.3 and 62.0 LPHH, which were observed on the images captured by cameras C1 and C2, both with FHD image-sensors. The highest camera resolution (65.3 LPHH) was observed in the image

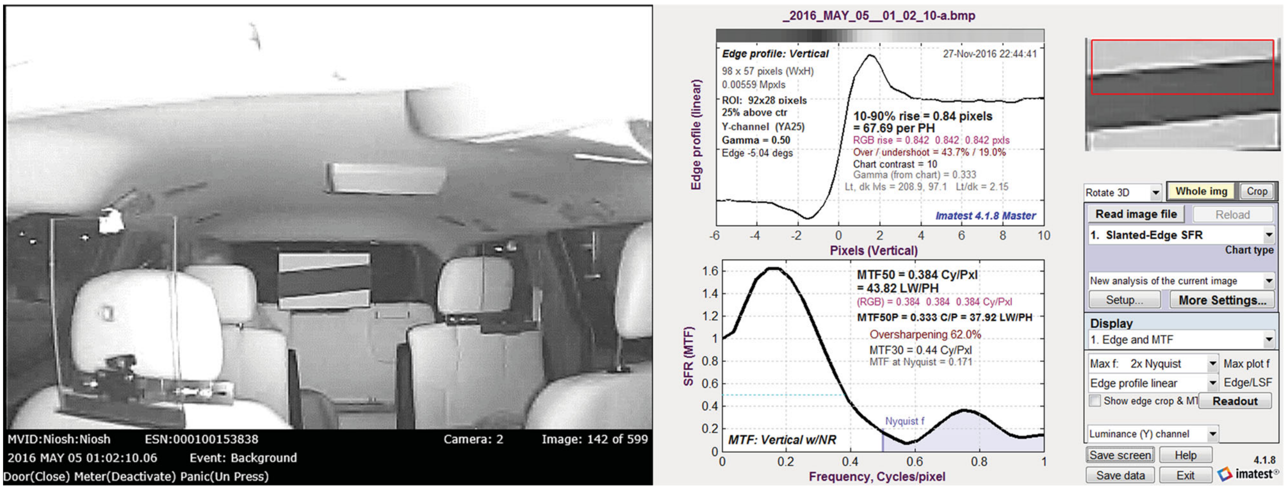

Figure 3. Video image captured by camera C4 (dual standard-definition image-sensors) and the resolution measurement charts. The SFR (MTF)–frequency chart shows a measured resolution of 37.9 LPHH, which is the spatial frequency as the MTF falls to 50% from its peak (MTF50P).
Note: The full color version of this figure is available online. ctr = center; C/P = cycles per pixel; Cy/Pxl = cycles per pixel; degs = degrees; LPHH = linewidths per head height; LSF = logarithmic frequency (simple); Lt/dk = light / dark; Lt, dk lvls = light, dark levels; LW/PH = linewidth per picture height; Max f = maximum frequency; Max plot f = maximum plot frequency; Mpxls = megapixels; MTF = modulation transfer function; MTF30 = spatial frequency where the system response is 30% of the baseline low frequency; MTF50 = spatial frequency where the system response is 50% of the baseline low frequency; MTF50P = spatial frequency where MTF drops from peak value to 50% of its baseline low frequency; Nyquist f = Nyquist frequency; PH = picture height; pxls = pixels; RGB = red–green–blue; ROI = region of interest; SFR = spatial frequency response; Vertical w/NR = vertical with noise reduction; W×H = width × height; Whole img = whole image.

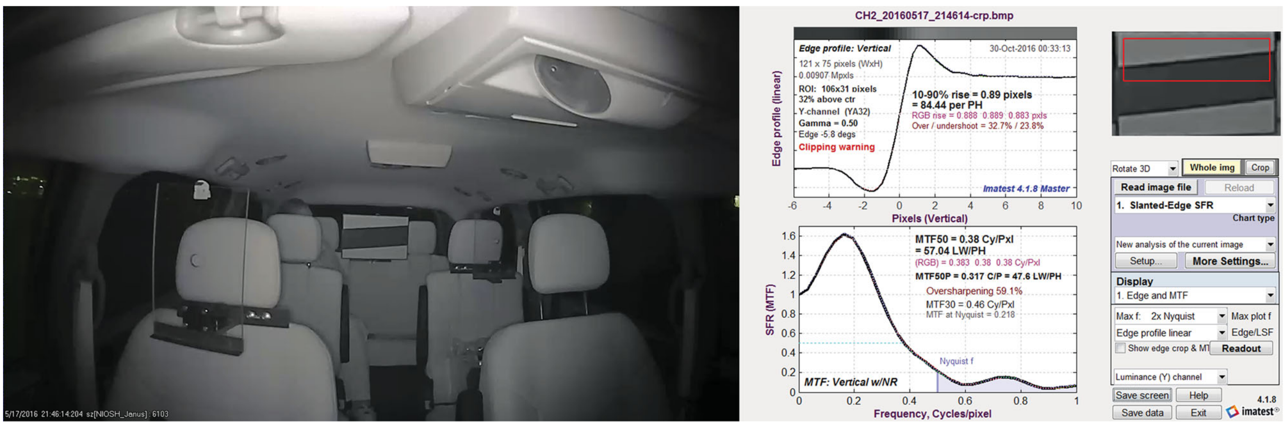

Figure 4. Video image captured by camera C3 equipped with a high-definition image-sensor. The SFR (MTF)–frequency chart shows a measured resolution of 47.6 LPHH, which is close to the camera resolution threshold for facial identification (47.7 LPHH).
Note: The full color version of this figure is available online. ctr = center; C/P = cycles per pixel; Cy/Pxl = cycles per pixel; degs = degrees; LPHH = linewidths per head height; LSF = logarithmic frequency (simple); Lt/dk = light / dark; Lt, dk lvls = light, dark levels; LW/PH = linewidth per picture height; Max f = maximum frequency; Max plot f = maximum plot frequency; Mpxls = megapixels; MTF = modulation transfer function; MTF30 = spatial frequency where the system response is 30% of the baseline low frequency; MTF50 = spatial frequency where the system response is 50% of the baseline low frequency; MTF50P = spatial frequency where MTF drops from peak value to 50% of its baseline low frequency; Nyquist f = Nyquist frequency; PH = picture height; pxls = pixels; RGB = red–green–blue; ROI = region of interest; SFR = spatial frequency response; Vertical w/NR = vertical with noise reduction; W×H = width × height; Whole img = whole image.

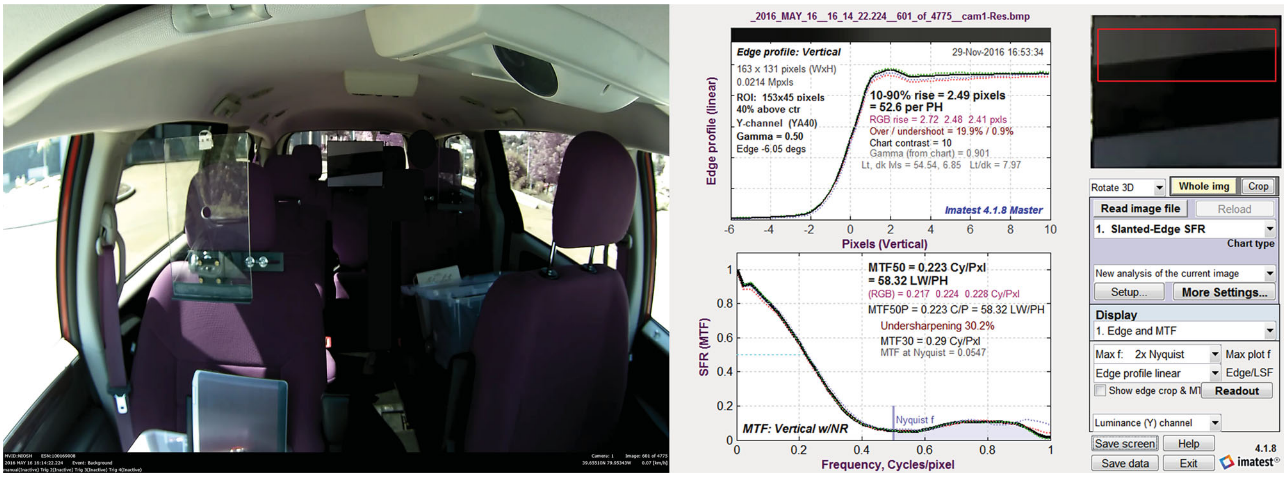

Figure 5. Video image captured by camera C1 equipped with a full high-definition image-sensor. The SFR (MTF)–frequency chart shows a measured resolution of 58.3 LPHH.
Note: The full color version of this figure is available online. ctr = center; C/P = cycles per pixel; Cy/Pxl = cycles per pixel; degs = degrees; LPHH = linewidths per head height; LSF = logarithmic frequency (simple); Lt/dk = light / dark; Lt, dk lvls = light, dark levels; LW/PH = linewidth per picture height; Max f = maximum frequency; Max plot f = maximum plot frequency; Mpxls = megapixels; MTF = modulation transfer function; MTF30 = spatial frequency where the system response is 30% of the baseline low frequency; MTF50 = spatial frequency where the system response is 50% of the baseline low frequency; MTF50P = spatial frequency where MTF drops from peak value to 50% of its baseline low frequency; Nyquist f = Nyquist frequency; PH = picture height; pxls = pixels; RGB = red–green–blue; ROI = region of interest; SFR = spatial frequency response; Vertical w/NR = vertical with noise reduction; W×H = width × height; Whole img = whole image.

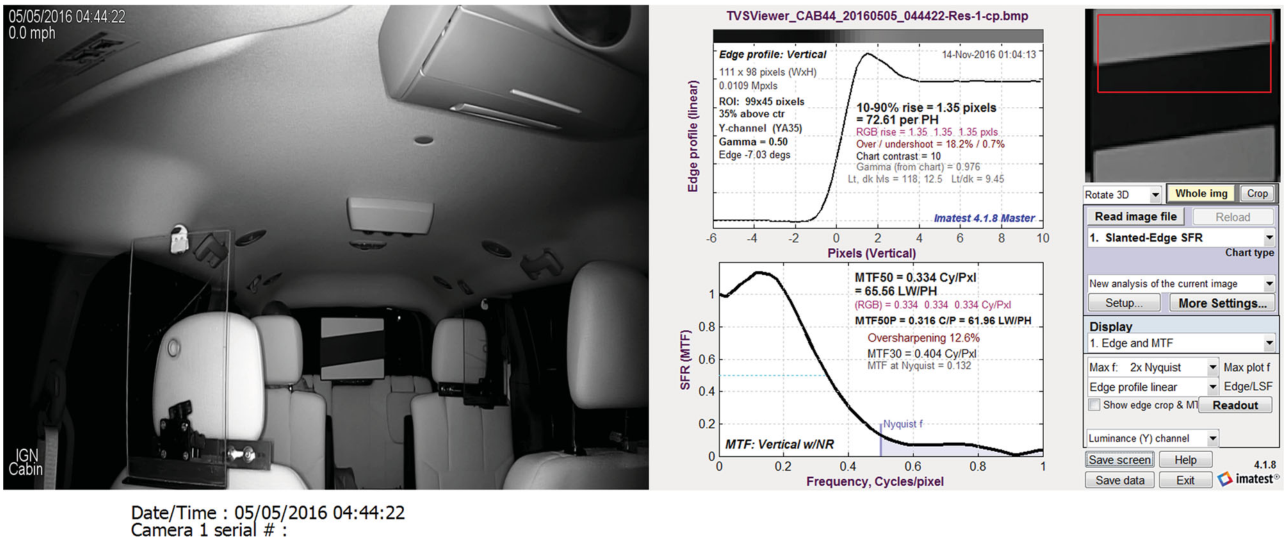

Figure 6. Video image captured by camera C2 equipped with a full high-definition image-sensor. The SFR (MTF)–frequency chart shows a measured resolution of 62.0 LPHH.
Note: The full color version of this figure is available online. ctr = center; C/P = cycles per pixel; Cy/Pxl = cycles per pixel; degs = degrees; LPHH = linewidths per head height; LSF = logarithmic frequency (simple); Lt/dk = light / dark; Lt, dk lvls = light, dark levels; LW/PH = linewidth per picture height; Max f = maximum frequency; Max plot f = maximum plot frequency; Mpxls = megapixels; MTF = modulation transfer function; MTF30 = spatial frequency where the system response is 30% of the baseline low frequency; MTF50 = spatial frequency where the system response is 50% of the baseline low frequency; MTF50P = spatial frequency where MTF drops from peak value to 50% of its baseline low frequency; Nyquist f = Nyquist frequency; PH = picture height; pxls = pixels; RGB = red–green–blue; ROI = region of interest; SFR = spatial frequency response; Vertical w/NR = vertical with noise reduction; W×H = width × height; Whole img = whole image.

captured by the dome camera of camera-group C5 with a standard-definition image-sensor, shown in Figure 7.

Table 2 presents the camera resolutions in both light conditions L1 and L2. The highest total-mean camera resolution is 60.9 LPHH, which was observed in the images captured by the dome camera of camera-group C5. The lowest total-mean camera resolution of 42.3 LPHH, which was observed in the images captured by camera C4, was below the camera resolution threshold for facial identification (47.7 LPHH). The dome-mounted camera maintains the highest mean camera resolution among the five cameras in condition L1, and an FHD windshield-mounted camera

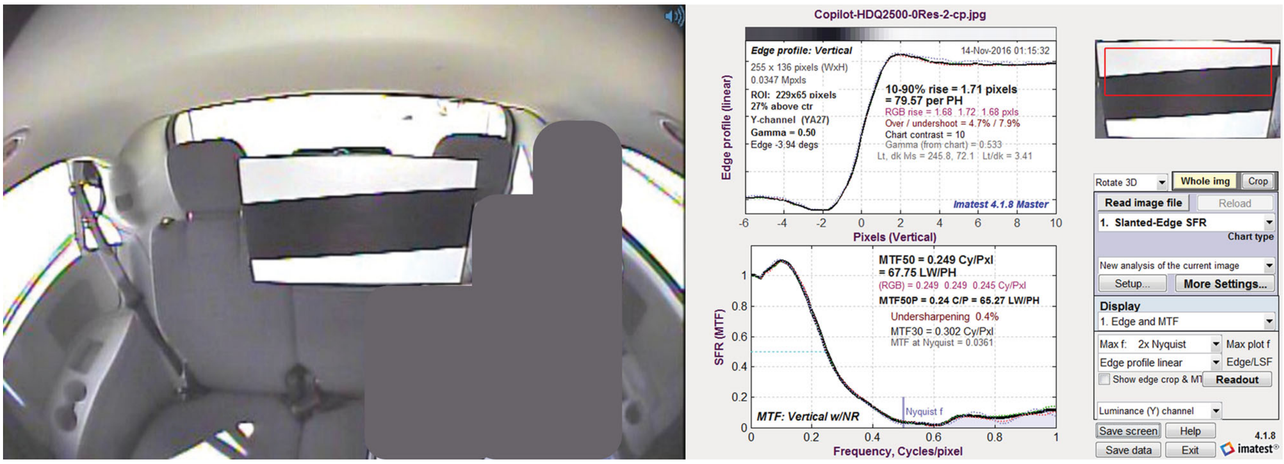

Figure 7. Video image captured by the dome camera of camera-group C5 with a standard-definition image-sensor. The SFR (MTF)–frequency chart shows a measured resolution of 65.3 LPHH, which is the highest camera resolution observed in the resolution tests.
Note: The full color version of this figure is available online. ctr = center; C/P = cycles per pixel; Cy/Pxl = cycles per pixel; degs = degrees; LPHH = linewidths per head height; LSF = logarithmic frequency (simple); Lt/dk = light / dark; Lt, dk lvls = light, dark levels; LW/PH = linewidth per picture height; Max f = maximum frequency; Max plot f = maximum plot frequency; Mpxls = megapixels; MTF = modulation transfer function; MTF30 = spatial frequency where the system response is 30% of the baseline low frequency; MTF50 = spatial frequency where the system response is 50% of the baseline low frequency; MTF50P = spatial frequency where MTF drops from peak value to 50% of its baseline low frequency; Nyquist f = Nyquist frequency; PH = picture height; pxls = pixels; RGB = red–green–blue; ROI = region of interest; SFR = spatial frequency response; Vertical w/NR = vertical with noise reduction; W×H = width × height; Whole img = whole image.

maintains the highest mean camera resolution in condition L2. Only the camera resolution of the dome-mounted camera in the third-row seats in the daylight (L1) condition was above the monochrome resolution threshold for computer facial recognition (64 LPHH).

Figure 8 shows two test chart images taken by camera C1 and their resolution measurement charts in light conditions L1 and L2. The video image (Figure 8a) captured in daylight (L1) conditions was clean without apparent speckles. Random speckles were observed in image (Figure 8b), which was captured in dark conditions with IR radiation. The camera resolution of camera C1 in condition L1 (58.3 LPHH) was 10.9 LPHH higher than that in condition L2 (47.4 LPHH, below the camera resolution threshold for facial identification).

4. Discussion

The highest total-mean camera resolution in the third-row seat (60.9 LPHH) was observed in the images captured by the dome camera of camera-group C5 with a standard-definition image-sensor of 976 × 494 pixels. This was attributed to the shorter distance between the dome camera and the test chart in the third-row seat (80 cm), which was 158 cm shorter than the distance between the windshield-mounted cameras and the test chart in the third-row seat (238 cm). The advantage of using a standard-definition dome camera is that it has a much smaller video data file size than that of HD and FHD cameras. A windshield-mounted FHD camera has similar camera resolution to that of a dome-mounted standard-definition camera in the third-row seats, but has a much larger data file size than that of a standard-definition dome camera. There would be a conflict between the use of FHD cameras in taxicabs and the long video retention period, up to 30 days, required by some city regulators and jurisdictions. The need for large data storage could significantly increase the cost of a taxicab security camera system with an FHD camera. A dome-mounted standard-definition camera solves this camera resolution–file size conflict problem. The other advantages of the dome camera are that there is no view blockage between a dome camera and the customers in the third-row seats, and the ambient lighting condition surrounding a dome camera is more uniform than that surrounding windshield-mounted cameras. The disadvantage of using a dome-mounted camera is that a camera group is needed for the camera system instead of a single camera in windshield-mounted camera systems. A single windshield-mounted FHD or HD camera also meets the camera resolution requirement for facial identification in three-row-seating taxicabs. The resolution of camera C4, with dual standard-definition image-sensors, in the third-row seats was below the camera resolution threshold for facial identification; therefore, the findings of this study indicate that windshield-mounted standard-definition cameras are not suggested for use in three-row-seating taxicabs.

The camera resolution threshold for computer facial recognition is 16.3 LPHH higher than that for facial identification. The dome-mounted standard-definition camera in only the daylight (L1) condition could meet the

Table 2. Camera resolution performance in LPHH (head height = 25.5 cm).

Camera		Camera 1 (FHD)			Camera 2 (FHD)			Camera 3 (high definition)			Camera 4 (dual standard definition)			Camera 5 (windshield–dome)		
		Light intensity			Light intensity			Light intensity			Light intensity			Light intensity		
Light condition	Measurement	Sun (×1k lx)	Third-row seat (lx)	Camera res. (LPHH)	Sun (×1k lx)	Third-row seat (lx)	Camera res. (LPHH)	Sun (×1k lx)	Third-row seat (lx)	Camera res. (LPHH)	Sun (×1k lx)	Third-row seat (lx)	Camera res. (LPHH)	Sun (×1k lx)	Third-row seat (lx)	Camera res. (LPHH)
Daylight (L1)	1	116.3	345	58.3	120.9	508.0	51.8	120.9	508.0	54.1	120.9	508.0	45.5	122.7	406.0	63.9
	2	116.1	346	57.3	120.9	510.0	52.6	120.9	510.0	54.7	120.9	510.0	45.8	122.7	407.0	65.3
	3	116.1	346	56.8	120.7	510.0	51.6	120.7	510.0	50.0	120.7	510.0	45.7	122.7	406.0	64.4
	4	116.2	346	58.5	120.8	511.0	51.7	120.8	511.0	54.9	120.8	511.0	45.0	122.8	405.0	64.5
	5	116.3	346	54.8	120.7	510.0	51.9	120.7	510.0	55.6	120.7	510.0	45.6	122.7	405.0	65.0
	Mean	–	–	57.1	–	–	51.9	–	–	53.9	–	–	45.5	–	–	64.6
	SD	–	–	1.5	–	–	0.4	–	–	2.2	–	–	0.3	–	–	0.6
		Sky (lx)	Third-row seat (IR) ($\mu W/cm^2$)	Camera res. (LPPH)	Sky (lx)	Third-row seat (IR) ($\mu W/cm^2$)	Camera res. (LPPH)	Sky (lx)	Third-row seat (IR) ($\mu W/cm^2$)	Camera res. (LPPH)	Sky (lx)	Third-row seat (IR) ($\mu W/cm^2$)	Camera res. (LPPH)	Sky (lx)	Third-row seat (IR) ($\mu W/cm^2$)	Camera res. (LPPH)
Dark with infrared (L2)	1	0.28	1.29	48.9	0.37	2.53	62.0	0.20	2.47	47.6	0.31	1.40	37.9	0.37	39.7	58.5
	2	0.28	1.29	47.3	0.36	2.54	61.6	0.22	2.49	49.2	0.32	1.42	39.7	0.36	39.7	56.7
	3	0.30	1.29	49.2	0.35	2.55	62.1	0.22	2.49	49.4	0.31	1.40	39.1	0.36	39.7	57.5
	4	0.29	1.29	49.8	0.36	2.54	61.6	0.22	2.48	50.1	0.35	1.40	38.4	0.36	39.7	56.6
	5	0.28	1.29	47.4	0.35	2.52	61.2	0.21	2.46	48.4	0.31	1.40	39.9	0.35	39.7	57.1
	Mean	–	–	48.5	–	–	61.7	–	–	48.9	–	–	39.0	–	–	57.3
	SD	–	–	1.1	–	–	0.4	–	–	1.0	–	–	0.8	–	–	0.7
L1 + L2	Total-mean	–	–	52.8	–	–	56.8	–	–	51.4	–	–	42.3	–	–	60.9
	SD	–	–	4.7	–	–	5.2	–	–	3.1	–	–	3.5	–	–	3.9

Note: ×1k lx = × 1000 lumen/m^2; Camera res. = normalized camera resolution; Dark with infrared (L2) = moonless dark with infrared radiation; Daylight (L1) = sunny daylight; FHD = full high definition; IR = with infrared radiation; L1 + L2 = both light conditions L1 and L2; LPHH = linewidths per head height; Sky = light intensity of the sky; Sun = light intensity of the sun.

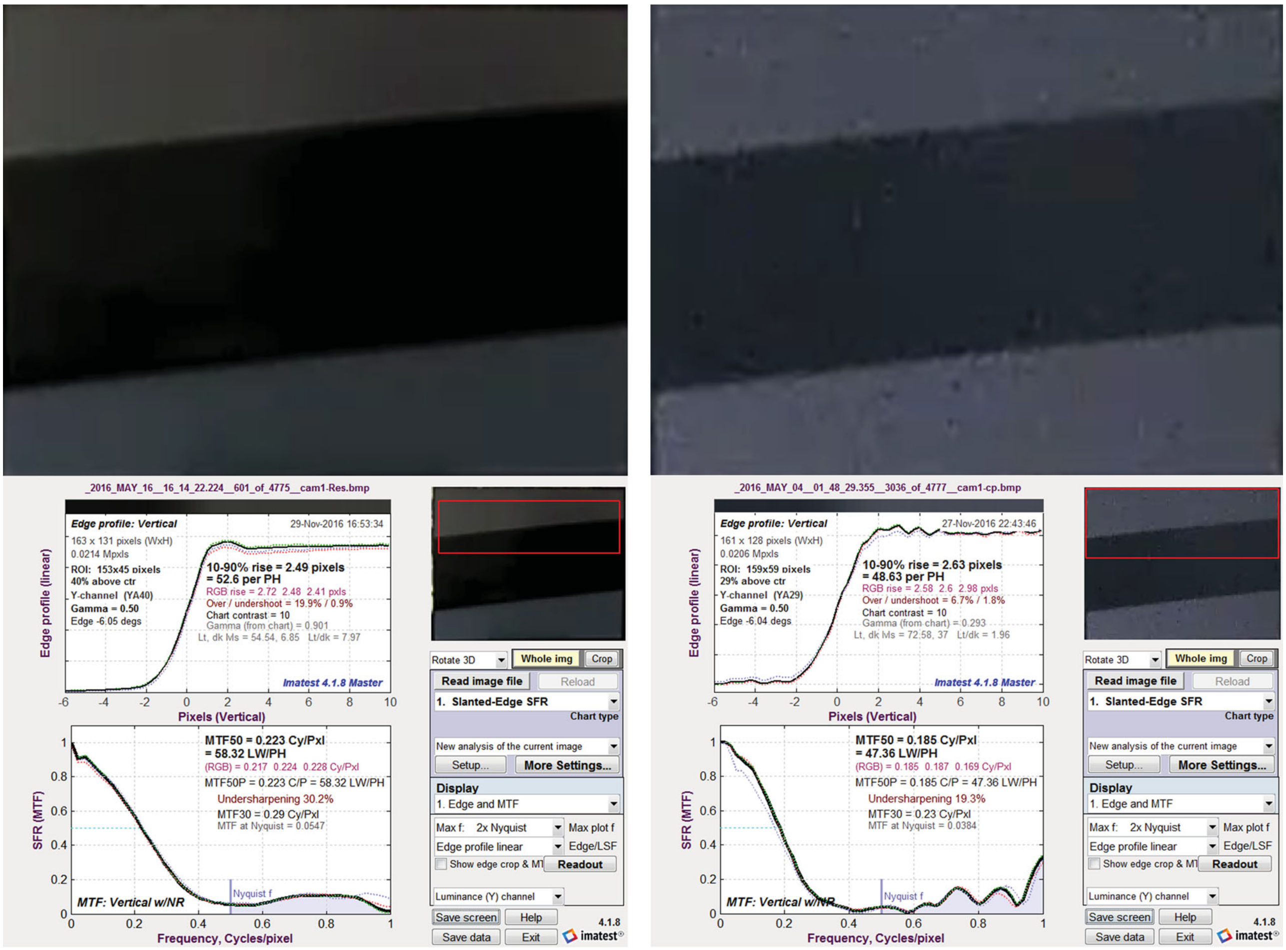

(a) (b)

Figure 8. Chart images captured by camera C1 (a) in the daylight condition and (b) in the dark condition with infrared radiation.
Note: The full color version of this figure is available online. ctr = center; C/P = cycles per pixel; Cy/Pxl = cycles per pixel; degs = degrees; LSF = logarithmic frequency (simple); Lt/dk = light / dark; Lt, dk lvls = light, dark levels; LW/PH = linewidth per picture height; Max f = maximum frequency; Max plot f = maximum plot frequency; Mpxls = megapixels; MTF = modulation transfer function; MTF30 = spatial frequency where the system response is 30% of the baseline low frequency; MTF50 = spatial frequency where the system response is 50% of the baseline low frequency; MTF50P = spatial frequency where MTF drops from peak value to 50% of its baseline low frequency; Nyquist f = Nyquist frequency; PH = picture height; pxls = pixels; RGB = red–green–blue; ROI = region of interest; SFR = spatial frequency response; Vertical w/NR = vertical with noise reduction; W×H = width × height; Whole img = whole image.

monochrome camera resolution requirement for computer facial recognition.

In Table 2, the mean camera resolution of camera C1 in daylight (L1) is 8.6 LPHH higher than in the dark (L2) condition. The resolution difference may be attributed to more random speckles in the images captured in condition L2 than those in condition L1. The random speckles are unwanted ‘image noise’ [23], which reduces the signal-to-noise ratio of the image, and hence reduces the image resolution [24]. In this case, the low-noise image-sensors may be needed in order to maintain camera resolution.

Future work includes seeking other solutions to camera noise reduction. Increasing the IR radiation intensity might reduce the number of speckles in facial images, and hence reduce the image noise in dark conditions.

5. Conclusions

A dome camera with a standard-definition image-sensor is suggested as an effective camera for maintaining high camera resolution with relatively small video data file size for facial identification in the third-row seats of three-row-seating taxicabs. Windshield-mounted security cameras with at least 1280 × 720 pixel image-sensors are also suggested for use for facial identification in three-row-seating taxicabs. Windshield-mounted security cameras with either single or dual standard-definition image-sensors are not suggested for use in three-row-seating taxicabs due to their low camera resolution in the third-row seats. Among the cameras under test, only the dome-mounted camera in the daylight condition could meet the monochrome camera resolution requirement for computer facial recognition. This study suggests the use of low-noise security cameras in order to maintain proper camera resolution in three-row-seating taxicabs.

Acknowledgements

The author would like to thank Mr Bradley Newbraugh and Ms Darlene Weaver for their assistance in experiment preparation and data collection. The author would like to thank Mr Nelson Barros and Dr Ian Radbone for their external peer reviews, and Dr Stephen Martin for his internal peer review. The author would also like to thank Mr James Green, Dr Hongwei Hsiao, Dr Tony McKenzie, Mr Frank Palya and Mr Timothy Pizatella for their internal reviews.

6. Disclaimers

The findings and conclusions in this report are those of the author and do not necessarily represent the official position of the National Institute for Occupational Safety and Health (NIOSH), Centers for Disease Control and Prevention. Mention of company names or products does not imply endorsement by the NIOSH.

Disclosure statement

No potential conflict of interest was reported by the author.

Funding

This research project was funded by Division of Safety Research, National Institute for Occupational Safety and Health, Centers for Disease Control and Prevention, USA [Grant Number: CAN9927875].

ORCID

Shengke Zeng http://orcid.org/0000-0003-4530-190X

References

[1] Bureau of Labor Statistics. Table A-6. Fatal occupational injuries resulting from transportation incidents and homicides, all United States, 2018. In: 2018 Census of Fatal Occupational Injuries. Washington (DC): Bureau of Labor Statistics; 2018. Available from: https://www.bls.gov/iif/oshwc/cfoi/cftb0327.htm

[2] Bureau of Labor Statistics. Table 18. Employed persons by detailed industry, sex, race, and Hispanic or Latino ethnicity. In: Labor Force Statistics from the Current Population Survey, 2018 annual averages – household data. Washington (DC): Bureau of Labor Statistics; 2018. Available from: https://www.bls.gov/cps/cpsaat18.pdf

[3] Menéndez CC, Amandus HE, Damadi P, et al. Effectiveness of taxicab security equipment in reducing driver homicide rates. Am J Prev Med. 2013;45(1):1–8. doi:10.1016/j.amepre.2013.02.017

[4] Zeng S, Amandus HE, Amendola AA, et al. Minimum requirements for taxicab security cameras. J Trans Technol. 2014;4(3):216–255. doi:10.4236/jtts.2014.43022

[5] Zeng S, Amandus HE, Amendola AA, et al. Evaluation of sample taxicab security cameras. J Trans Technol. 2017;7(4):390–422. doi:10.4236/jtts.2017.74026

[6] Ministry of Transport. Taxi industry safety and security taskforce final report. Sydney (NSW): Ministry of Transport; 2007. Available from: http://www.tda.net.au/taxi-safety-taskforce-final-report.pdf

[7] New South Wales Taxi Council. NSW Taxi driver guide to a safer workplace. Sydney (NSW): New South Wales Taxi Council; 2007.

[8] New York City Taxi & Limousine Commission. Taxi cab notes 4.23.2000 v1.b. Taxi & Limousine Commission, March 2000 Press Release, Industry Notice #00-08. New York (NY): Taxi & Limousine Commission; 2000. Available from: http://www.mediaeater.com/cameras/news/taxi.html

[9] Ramzan S, Christian A. Report of the Sheffield taxi safety camera pilot study, Sheffield Taxi Camera Safety Project 1. Sheffield: Sheffield City Council, Neighbourhoods and Community Care Directorate, Regeneration and Partnership, Policy Support Unit; 2007. Available from: https://www.whatdotheyknow.com/request/149947/response/369138/attach/3/1%20Report%20Draft%20V10.pdf

[10] Tasmanian Office of Parliamentary Counsel. Taxi industry amendment (security cameras) regulations 2004 (S.R. 2004, No. 21). Hobart (TAS): Office of Parliamentary Counsel; 2004. Available from: http://www5.austlii.edu.au/au/legis/tas/num_reg/tiacr20042004n21609/

[11] Transport Certification Australia. Queensland taxi security camera specifications. Melbourne (VIC): Transport Certification Australia; 2006.

[12] Victoria Government Gazette. Specifications for taxi-cab security cameras. Melbourne (VIC): Authority of Victorian Government; 2016. Available from: https://www.victaxi.com.au/assets/downloads/Taxicab%20Camera%20Specifications%20-%2023%20Dec%2016.pdf

[13] Human Factors Engineering Technical Advisory Group. Human engineering design data digest, human factors standardization subtag. Washington, DC: Human Factors Engineering Technical Advisory Group, Departmentof Defense, USA; 2000. p. 82. Available from: https://rt.cto.mil/wp-content/uploads/2019/07/HE_Design_Data_Digest-acts.pdf

[14] Wang J, Zhang C, Shum HY. Face image resolution versus face recognition performance based on two global methods. Paper presented at IEEE 6th Asian Conference on Computer Vision (ACCV); Jan 2004; Jeju Island. Available from: https://pdfs.semanticscholar.org/f1aa/45b50a86e88fae91a91e5df18f3e7c43894f.pdf

[15] image-engineering.us [Internet]. Resolution measurement and its units. South Lake Tahoe (CA): Image Engineering. c1995–2020; 2011 May 20 [cited 2020 Jun 4]; [about 2 screens]. Available from: https://www.image-engineering.de/library/technotes/761-resolution-measurement-and-its-units

[16] Burns PD. Slanted-edge MTF for digital camera and scanner analysis. In: Proceedings of the IS&T 2000 PICS Conference, 2000 March, Portland (OR), USA. Springfield (VA): Society for Imaging Science & Technology; 2000. p. 135–138. Available from: http://www.losburns.com/imaging/pbpubs/26pics2000burns.pdf

[17] imatest.com [Internet]. Sharpness: what is it and how is it measured? Boulder (CO): Imatest LLC; c2004–2020 [cited 2020 Jun 04]; [about 6 screens]. Available from: http://www.imatest.com/docs/sharpness/

[18] Williams D. Benchmarking of the ISO 12233 slanted-edge spatial frequency response plug-in. In: IS&T's 1998 PICS Conference; 1998 May; Portland (OR). Springfield (VA): Society for Imaging Science & Technology. p. 133–136. Availablefrom: http://www.imagescienceassociates.com/mm5/pubs/Benchmarking_of_the_ISO_12233_Slanted-edge.pdf

[19] Ben-Ezra M. High resolution large format tile-scan camera: design, calibration, and extended depth of field.

Paper presented at 2010 IEEE International Conference on Computational Photography (ICCP), 29–30 March 2010, Cambridge (MA), USA. IEEE Xplore; 2010. doi:10.1109/ICCPHOT.2010.5585095

[20] Jenkin RB, Jacobson RE, Richardson MA, et al. Extension of the ISO 12233 SFR measurement technique to provide MTF bounds for critical imaging arrays. Proc SPIE-Int Soc Opt Eng. 2005;5668:129–137. doi:10.1117/12.593081

[21] Koren N. The Imatest program: comparing cameras with different amounts of sharpening. In: Proceddings of SPIE 6069, Digital Photography II, 60690L; 2006 Feb 10, Electronic Imaging, 15–19 January 2006, San Jose (CA), USA. Bellingham (WA): SPIE (the international society for optics and photonics). doi:10.1117/12.650848

[22] Triantaphillidou S, Jacobson RE. Measurements of the modulation transfer function of image displays. J Imaging Sci Technol. 2004 Feb;48(1):58–65. Available from: https://westminsterresearch.westminster.ac.uk/download/0ee09151de45f2358337af08a34615a410c3b2728588249f849d4287c90eafd6/536161/Triantaphillidou_Jacobson_2004_final.pdf

[23] Boyat AK, Joshi BK. A review paper: noise models in digital image processing. Signal Image Process Int J. 2015 Apr;6(2):arXiv: 1505.03489. Available from: https://arxiv.org/ftp/arxiv/papers/1505/1505.03489.pdf

[24] Treibitz T, Schechner Y. Resolution loss without imaging blur. J Opt Soc Am A. 2012;29(8):1516–1528. doi:10.1364/JOSAA.29.001516